

Graphene Nanoribbon-based Synapses with Versatile Plasticity

Wang, H.; Cucu Laurenciu, N.; Jiang, Y.; Cotofana, S.D.

DOI

[10.1109/NANOARCH47378.2019.181301](https://doi.org/10.1109/NANOARCH47378.2019.181301)

Publication date

2020

Document Version

Final published version

Published in

2019 IEEE/ACM International Symposium on Nanoscale Architectures (NANOARCH)

Citation (APA)

Wang, H., Cucu Laurenciu, N., Jiang, Y., & Cotofana, S. D. (2020). Graphene Nanoribbon-based Synapses with Versatile Plasticity. In *2019 IEEE/ACM International Symposium on Nanoscale Architectures (NANOARCH)* (pp. 1-6). Article 9073307 IEEE. <https://doi.org/10.1109/NANOARCH47378.2019.181301>

Important note

To cite this publication, please use the final published version (if applicable). Please check the document version above.

Copyright

Other than for strictly personal use, it is not permitted to download, forward or distribute the text or part of it, without the consent of the author(s) and/or copyright holder(s), unless the work is under an open content license such as Creative Commons.

Takedown policy

Please contact us and provide details if you believe this document breaches copyrights. We will remove access to the work immediately and investigate your claim.

Graphene Nanoribbon-based Synapses with Versatile Plasticity

H. Wang, N. Cucu Laurenciu, Y. Jiang, S.D. Cotofana
Computer Engineering Laboratory,

Delft University of Technology, The Netherlands.

{H.Wang-13, N.CucuLaurenciu, Yande.Jiang, S.D.Cotofana}@tudelft.nl

Abstract—Designing and implementing artificial systems that can be interfaced with the human brain or that can provide computational ability akin to brain’s processing information efficient style is crucial for understanding human brain fundamental operating principles and to unleashing the full potential of brain-inspired computing. As basic neural network components, responsible for information transfer between neurons, artificial synapses able to emulate analog biological synaptic behaviour are of particular interest. State of the art CMOS and memristor-based synapses suffer from scalability drawbacks (large energy consumption and area footprint), variability-induced instability, and are not bio-compatible. In this paper, we propose a generic Graphene Nanoribbon (GNR) based synapse structure and demonstrate that by changing GNR geometry and external bias voltages it can emulate different synaptic plasticity behaviours, i.e., Spike Timing Dependent Plasticity and Long-Term Depression and Potentiation, and that both excitatory and inhibitory synaptic behavior can be obtained with the same GNR geometry. To demonstrate biologically plausible operation, we make use of low voltage bias, i.e., 0.1 V, 0.2 V, and consider inputs consistent with measured brain synapses data, i.e., -50 mV to 50 mV pre- and post-synaptic spikes voltage range, and -60 ms to 60 ms time range. The simulations indicate that by changing the GNR shape we can enrich the plasticity behaviour (potentially beyond the considered cases) and the plasticity change of 100% provided by natural synapses can be achieved. Our investigation clearly suggests that the proposed GNR synapse structure is a promising candidate for large-scale neuromorphic systems integration, which might potentially bring novel insight on brain neurophysiology, as it requires a small footprint, is energy effective, biocompatible, and versatile from the synaptic behaviour point of view.

Index Terms—Neuromorphic Computing, STDP, Artificial Synapse, Graphene, GNR.

I. INTRODUCTION

The human brain, comprising approximately 86 billion neurons connected through trillions of synapses, is the natural high performance computing system. Its unique capabilities, e.g., low power consumption, robustness, massively parallel information processing, suitability for complex tasks, inspired Carver Mead in the late 1980s [1] in coining a disruptive computing paradigm, the Neuromorphic Computing (NC). Over the last decades NC gained substantial momentum, provided valuable insight into brain’s complex functionality, novel brain-inspired computation paradigms have been introduced [2], and biologically-inspired neuromorphic systems fabricated [3].

Synapses are the most ubiquitous neural system components which are ensuring information interchange between neurons. Their essential property is Synaptic Plasticity (SP), manifested either by the strengthening or the weakening of the transmitted signals, is the brain learning and memory

enabler. Spike Timing Dependent Plasticity (STDP), which enables synaptic transmission strength changes according to the relative timing of pre- and post-synaptic spikes, Long-Term Potentiation (LTP) and Long-Term Depression (LTD), which are persistent synaptic strengthening and weakening, respectively, are the essential functionalities an artificial synapse ought to be endowed with [4].

Given that at any brain inspired system crux of the matter reside artificial synapses able to emulate the biological ones, their design and fabrication received massive attention. In most of today’s neuromorphic computing systems, artificial synapses are typically implemented using dozens of CMOS devices [5], [6]. However, CMOS technology inadvertently imposes restrictions on both functionality and neuromorphic system implementations, foremost in terms of energy efficiency, scalability, and integration density. Furthermore, CMOS devices cannot truly convey the analog behaviour associated with biological synapses. Alternatively, emerging resistive switching memory devices [7] based synapses have been also proposed [8], [9] and exhibit promising characteristics, e.g., simple (a single or a few memristors) structure, inherently analog conductance, and good scalability potential. However, they suffer from temporal (cycle-to-cycle) and spatial (device-to-device) variability of the resistive state even under the same applied signals, as well as undesired nonlinearities, which may cause the instability of the entire neuromorphic system.

Graphene, one of the prominent post-Si forerunners, owing to its outstanding properties, e.g., fast switching speed, low energy, thermal stability, ultimate thinness, flexibility, and biocompatibility [10], [11], has emerged as a potent material [12] and previous work demonstrated that graphene-based artificial synapse can emulate plasticity. In [13], by changing the back-gate voltage, the authors obtained various synaptic plasticities within the same device. However, quite large back-gate voltages (20 V, 40 V) and input pulses (2 V) are utilized, which are faraway larger than the electric potentials measured in natural neurons, and are negatively affecting the power consumption. Moreover, the obtained synaptic weight change is relatively small ($\approx 10\%$) when compared with (100%) in biological counterparts, and the provided synaptic plasticity is restricted. In [14], a fabricated graphene-based electrochemical synapse is reported, whose conductance is modulated by changing the Li ion concentration between the graphene layers. This synapse enables low-power switching, exhibits low variability, and is potentially suitable for large-scale integration. However, the reported STDP conductance change of $\approx 2\%$ and timing difference around 1000 ms are in

a different range than the one of natural synapses, i.e., $\approx 100\%$ and 100 ms, respectively.

In this paper, we propose a generic Graphene Nanoribbon (GNR) based synapse structure consisting of a GNR monolayer placed above an insulator and a doped substrate. Two top contacts are utilized to bias the GNR and its conduction modulated by means of electrostatic interaction via top and back gates reflects the synaptic weight. Specifically, we consider 2 fundamental synapse functionalities, i.e., Spike Timing Dependent Plasticity (STDP) and Long-Term Plasticity (LTP), which are known to underlie learning and memory in brain. By carving the GNR synapse geometry and changing the bias and back-gate voltages we successfully emulate: Balanced Hebbian STDP, Potentiation Dominated Hebbian STDP, Potentiation Dominated Anti-Hebbian STDP, and Long-Term Plasticity. Furthermore, we demonstrate that both excitatory and inhibitory synaptic behaviours can be obtained with the same GNR synapse, simply by changing the bias back-gate voltage. To demonstrate biologically plausible operation, we bias the GNRs at low voltage (0.1 V, 0.2 V) and consider inputs consistent with measured brain synapses data, i.e., -50 mV to 50 mV pre- and post-synaptic spikes voltage range, and -60 ms to 60 ms time range.

The simulations indicate that by changing the GNR shape we can enrich the plasticity behaviour (potentially beyond the 4 considered cases) and the plasticity change of 100% provided by natural synapses can be achieved. Our investigation clearly suggests that the proposed GNR synapse structure is a promising candidate for large-scale neuromorphic systems integration, which might potentially bring novel insight on brain neurophysiology, as it is small (e.g., 38 nm²), energy effective, biocompatible, and versatile from the synaptic behaviour point of view.

The remaining of this paper is organized as follows: Section II outlines basic synapse and plasticity concepts, and introduces the proposed GNR-based synapse. In Section III we describe the simulation model employed for simulating the GNR electronic properties, and the overall simulation setup and methodology. In Section IV we present the obtained simulation results, and in Section V we conclude the paper.

II. SYNAPTIC PLASTICITY AND GRAPHENE-BASED SYNAPSE

In this section, we briefly present the synaptic plasticity underlying concepts and then introduce the proposed graphene-based synapse.

To explain the role of a synapse in the neuron information interchange, Figure 1 depicts a very small network composed of two neurons, N_j and N_k , connected via synapses to a third neuron, N_i . Neuron N_i collects input signals from the two pre-synaptic neurons, N_j and N_k , and when their cumulated signals effects exceed a certain neuron-specific firing threshold, neuron N_i generates an output signal (spike) which then propagates through all its terminations. From the synapse perspective, (consider for instance the synapse between neurons N_i and N_j), there are (i) two input spikes: the

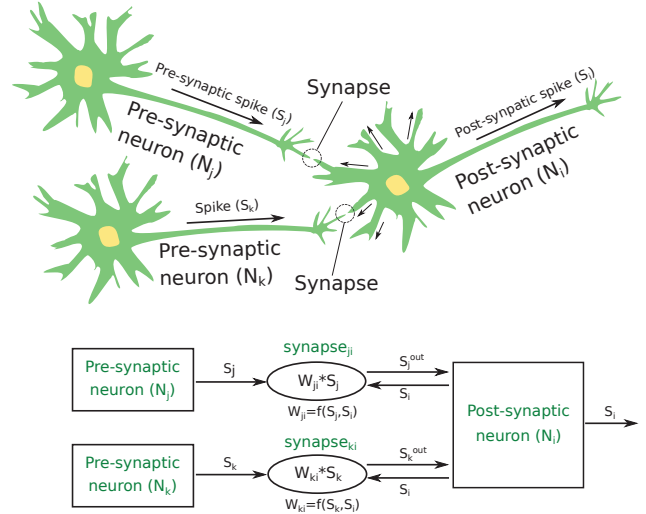


Fig. 1: Synaptic-based information interchange.

pre-synaptic spike S_j , which comes from neuron N_j , and the post-synaptic spike S_i , which is generated by neuron N_i , and (ii) one output spike S_j^{out} , which will be transmitted to neuron N_i . In general, the synaptic transmission efficiency - quantified through the synaptic weights W - is variable, either weakening or strengthening the magnitude of the signals transmitted via the synapse. This property is known as synaptic plasticity and it is believed to hold a crucial role in learning and memory in brain. Spike Timing Dependent Plasticity (STDP) [15] is a widely utilized Hebbian synaptic learning rule, for which the synaptic weight changes based on the relative timing between the pre- and post-synaptic spikes, as follows: (i) when the pre-synaptic spike arrives shortly prior to the post-synaptic one, the synaptic weight increases and this may lead to a persistent weight increase (Long-Term Potentiation (LTP)); otherwise, the synaptic weight decreases and may lead to a persistent weight decrease (Long-Term Depression (LTD)), and (ii) if the pre- and post-synaptic spikes arrive very close to each other, a large synaptic weight change occurs. We denote by ΔW , the synaptic weight change, and by $\Delta t = t_{post} - t_{pre}$, the arrival time difference of the pre- and post-synaptic spikes. Figure 2 graphically illustrates $\Delta W(\Delta t)$ according to a biological synapse measured data [16]. Even though the data exhibit stochasticity, a widely accepted interpolating model is the following:

$$\Delta W(\Delta t) = \begin{cases} A_+ \cdot \exp(-\Delta t/\tau_+), & \text{for } \Delta t > 0 \\ -A_- \cdot \exp(\Delta t/\tau_-), & \text{for } \Delta t < 0, \end{cases} \quad (1)$$

where A_+ and A_- are parameters determining the magnitude of synaptic potentiation and depression, while τ_+ and τ_- are time constants in the order of 10 ms fitted by experimental data reflecting the temporal range over which the synaptic strengthening and weakening occurs.

Figure 3 illustrates the proposed graphene-based generic synapse structure. It consists of a monolayer Graphene Nanoribbon (GNR) located above an insulating layer and

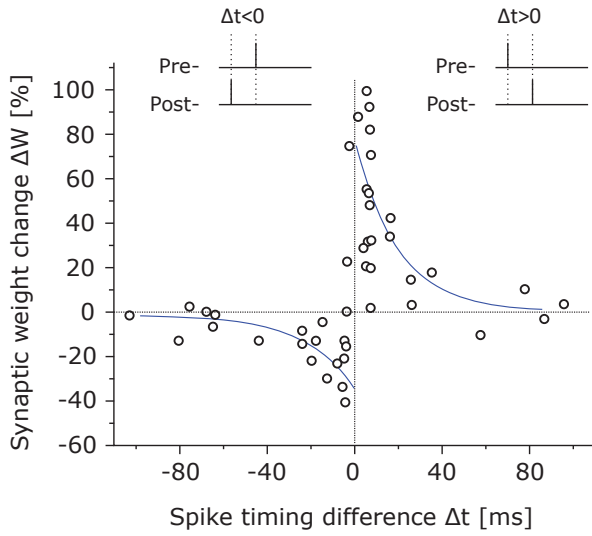


Fig. 2: Biological synapse STDP measured data [16].

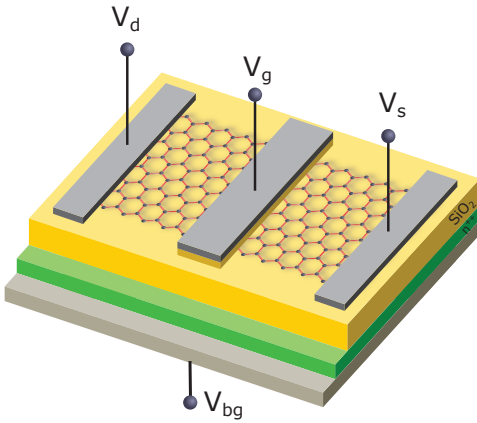


Fig. 3: Graphene-based synapse.

a doped substrate, which serves as back-gate. The GNR constitutes a conduction channel when applying a bias voltage $V_d - V_s$ between the source and the drain contacts and its conductance G can be modulated by the input voltage V_g applied on the top-gate. From the synapse operational standpoint, the top-gate is used for applying the synaptic input signals, the plasticity is reflected in the GNR conductance change, and the drain-to-source current is the synapse output current, which corresponds to the synaptic output spike S_j^{out} in Figure 1. When applying an input spike, which can be regarded as a time varying voltage, the synapse output current magnitude will depend on the cumulated previous activities in the synapse (for all the discrete voltages corresponding to the input spike). This dependence is accounted for in GNRs via a hysteretic I - V behaviour (specifically drain-to-source current vs. top-gate voltage), which is usually caused by defects in the top-gate oxide, that trap and release GNR carriers [17]. In the following we demonstrate that, different from previous graphene based synapse proposals, we can accommodate various plasticity types, by shaping the GNR

in non-rectangular forms. Furthermore, by tuning the back-gate voltage properly, both excitatory and inhibitory synapses can be implemented with the same graphene-based synapse.

III. SIMULATION FRAMEWORK

In this section, we present the model we used for deriving the electronic properties of the graphene synapse, and describe the simulation setup and the employed methodology to calculate the synaptic weight change (the GNR conductance change) and to obtain the plasticity behaviour.

A. Simulation Model

For the electronic transport computation, we used an NEGF-based hysteresis-aware simulation model [17]. Tight Binding (TB) Hamiltonian matrix $H = H_0 + U$ is used in this model to model the interaction between carbon atoms (via H_0) and external potentials (via U). The interaction matrix is calculated as follows:

$$H_0 = \sum_{i,j} t_{i,j} |i\rangle \langle j|, \quad (2)$$

$$\text{where } t_{i,j} = \begin{cases} \tau, & \text{if atoms } i \text{ and } j \text{ are adjacent} \\ 0, & \text{otherwise.} \end{cases} \quad (3)$$

We account for the first nearest-neighbor interaction with $\tau = -2.7eV$. The potential distribution U is calculated by solving a 3D Poisson equation self-consistently with finite difference method. As the interface traps cause an equivalent shift of the gate voltage, denoted ΔV_g , we update the potential profile with $V_g + \Delta V_g$ while solving the Poisson equation. The interface trap charge can be calculated with an accumulation equation:

$$Q_{it} = \sum \alpha_i \cdot Q_q \cdot \exp(-(t - t_{arrival})/t_{trap}), \quad (4)$$

where $t_{arrival}$ is the input spike arrival time. The value of α can be calculated as a function of the interface traps capacitance C_{it} :

$$\alpha(C_{it}) = \frac{C_{it} \cdot (V_g C_{ox} - Q_q)}{Q_q \cdot (C_{it} + C_{ox})}, \quad (5)$$

where V_g is the top-gate voltage, Q_q is quantum capacitor charge, C_{ox} is the oxide capacitance, and C_{it} is the interface traps capacitance, expressed as a function of the traps density as $C_{it} = q^2 \cdot D_{it}$.

The source and drain contacts along the end sides of graphene channel, which sustain the conduction, can be modeled with self-energy matrices Σ_1 and Σ_2 , respectively. Thus, the transmission function $T(E)$ that models the possibility of one electron being transmitted between the source and drain contacts, can be derived as a function of energy:

$$T(E) = \text{Trace} \left[\Gamma_1 G_R \Gamma_2 G_R^\dagger \right], \quad (6)$$

where

$$G_R(E) = [EI - H - \Sigma_1 - \Sigma_2]^{-1}, \quad (7)$$

$$\Gamma_{1,2} = i[\Sigma_{1,2} - \Sigma_{1,2}^\dagger]. \quad (8)$$

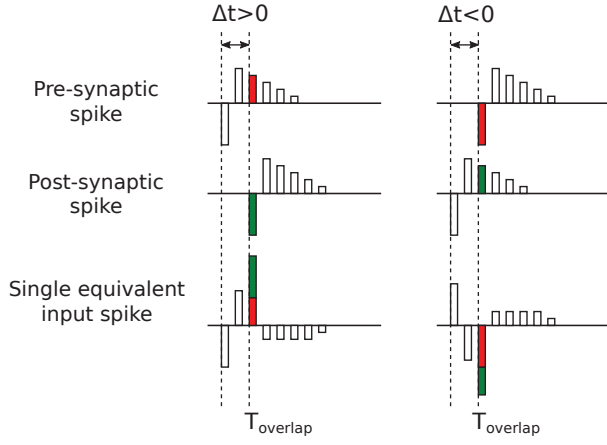


Fig. 4: Synapse single input spike scheme.

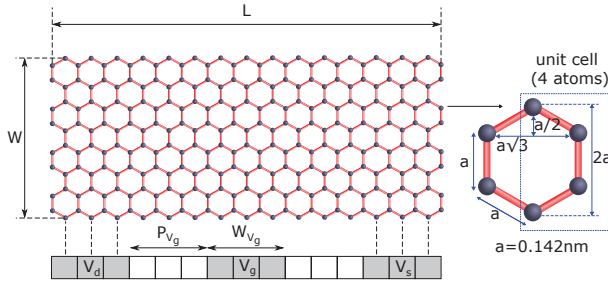


Fig. 5: GNR dimensions and contacts topology.

The current through the graphene channel is calculated by Landauer formula:

$$I = \frac{q}{h} \int_{-\infty}^{+\infty} T(E) \cdot (f_0(E - \mu_1) - f_0(E - \mu_2)) dE, \quad (9)$$

where $f_0(E)$ denotes the Fermi-Dirac distribution function at temperature T , and $\mu_{1,2}$ represents the source and drain contacts electrochemical potential. A block-by-block algorithm [18] for computing matrix inversion is used to speedup the calculation of G_R . Then the conductance of GNR device is calculated as:

$$G = \frac{I}{V_d - V_s}. \quad (10)$$

B. Simulation Setup and Methodology

In order to apply the input spikes to the graphene synapse, we employ a single-input scheme, as exemplified in Figure 4. The signal applied as input to the synapse is computed as a superposition of the pre- and post-synaptic spikes (i.e., the voltage difference between the two spikes). We define T_{overlap} as the arrival time of the secondly arriving spike. To perform biologically plausible simulations, we considered data consistent with measured data from brain synapses: -50 mV to 50 mV pre- and post-synaptic spikes voltage range, and -60 ms to 60 ms Δt range (which covers the general time range for biological LTP and LTD) [15], [16].

As concerns the GNR, we define its topology in Figure 5. In particular, W and L represent the GNR width and

length, P_{V_g} signifies the distance between the top-gate and the drain contact, and W_{V_g} denotes the width of the top-gate contact. In our simulation, we considered multiple non-rectangular GNRs with different shapes but the same overall $W = 39a$ and $L = 28\sqrt{3}a$. For the top-gate contact we set $P_{V_g} = 8\sqrt{3}a$ and $W_{V_g} = 6\sqrt{3}a$, where a is 0.142 nm. Concerning the traps induced hysteresis, we assume a density of interface traps of $2.5 \times 10^{-12} \text{cm}^{-2}(\text{eV})^{-1}$, and we set a trapping/detrapping time constant of 20 ms. Subsequently, we present the overall design and simulation methodology. For a desired plasticity behaviour, we first determine a potentially appropriate GNR geometry and drain-to-source and back-gate voltages. Subsequently, we subject the graphene synapse to a train of spikes applied via the top-gate, one spike for each Δt in the considered range. Corresponding to each input spike, we then measured the synaptic weight change ΔW (the difference between the GNR conductance values at two consecutive time moments, i.e., T_{overlap} and the immediately previous time moment), and assess its compliance with the desired $\Delta W(\Delta t)$ plasticity curve. If results are not according with the desired plasticity we change the GNR geometry and bias voltages.

IV. SIMULATION RESULTS

To evaluate the capabilities of proposed graphene synapse, we target 3 common plasticity types underlying balanced and potentiation dominated learning [19], [20]: Hebbian STDP with balanced LTD and LTP (Figure 6 (a)), LTP-biased Hebbian STDP (Figure 6 (d)), and LTP-biased Anti-Hebbian STDP (Figure 6 (g)).

Figure 6 (b) depicts the GNR synapse shape we obtained for the Hebbian STDP with balanced LTD and LTP scenario, biased at $V_d = 0.2$ V and back-gate voltage $V_{\text{back}} = 0.2$ V. The simulated synaptic weight change (conductance change) (Figure 6 (c)) indicates a good resemblance with the Hebbian STDP with balanced LTD and LTP weight change trend. In biological models, there is a certain randomness in the synapse reaction. We seek a synaptic reaction tendency closer to the plasticity models. When fitting the simulated conductance change with the canonical model in Equation 1, we obtained $\tau_+ = 23$ ms and $\tau_- = 37$ ms. Since for a biologically plausible input, we obtain an amplitude of the conductance change around 100%, which is consistent with biological synapse measured data shown in Figure 2, the proposed graphene synapse can enable potentially biologically plausible implementations (artificial synapses which can be interfaced with biological neurons in the context of, e.g., neural prosthetics).

Figure 6 (e) and (h) illustrate the obtained GNR synapse shapes for LTP-biased Hebbian STDP and LTP-biased anti-Hebbian STDP, respectively. The drain voltage V_d is set to 0.1 V for both shapes, while the applied back-gate voltage is 0 V and -0.5 V, respectively. The simulated synaptic weight change (conductance change) in Figure 6 (f) and (i) is temporally asymmetric, being dominated by (LTP) potentiation for both graphene synapses. When fitted with the model in Equation 1, we obtained $\tau_+ = 21$ ms and $\tau_- = 10$ ms for the

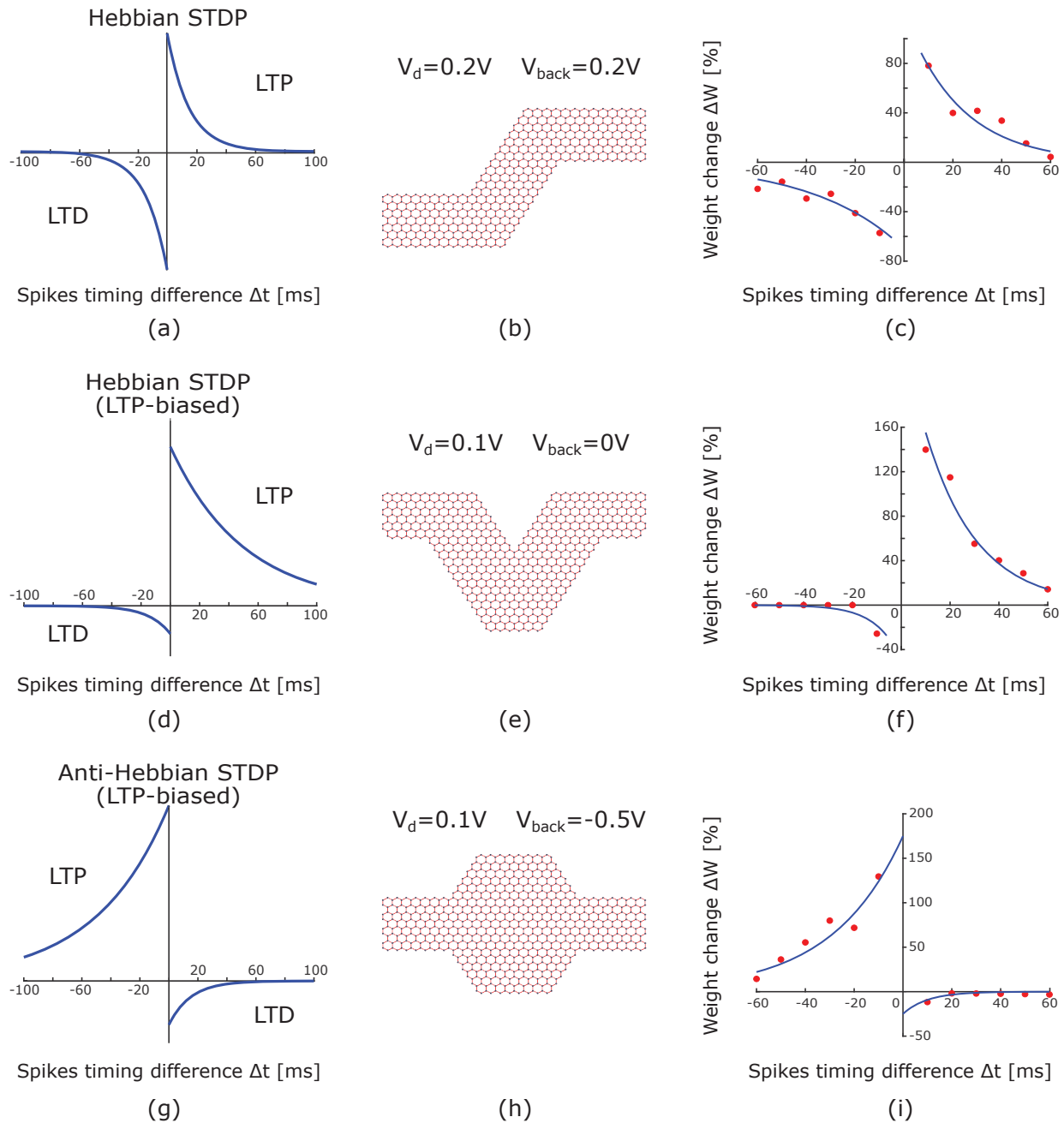


Fig. 6: GNR synapse shapes and corresponding STDP.

LTP-biased Hebbian synapse, and $\tau_+ = 19$ ms and $\tau_- = 15$ ms for the LTP-biased Anti-Hebbian synapse.

A synapse can either be excitatory (i.e., potentiation for pre-before-post synaptic spikes arrival) or inhibitory (i.e., depression for pre-before-post synaptic spikes arrival). Traditionally, 2 artificial synapses are employed, but we are able to obtain both excitatory and inhibitory behaviours with a single synapse, which is beneficial from the area and energy standpoints for large-scale integrations. For instance, the GNR synapse shape illustrated in Figure 6 (b) exhibits an excitatory behaviour but by simply changing the biasing gate voltage

V_{back} from 0.2 V to 0.5 V, while the other GNR applied voltages (V_d and V_g) are identical the inhibitory counterpart is obtained, as depicted in Figure 7.

Apart from STDP, Long-Term Plasticity is a fundamental synaptic functionality, dominant for how the brain stores information, which is obtained when applying an identical spike consecutively. In our experiments we considered the GNR synapse shape from Figure 6 (h) and applied 50 mV input spikes with an intermission period between the spikes of 1 s. For each spike, we measured the GNR drain to source current, which represents the current of the output spike generated

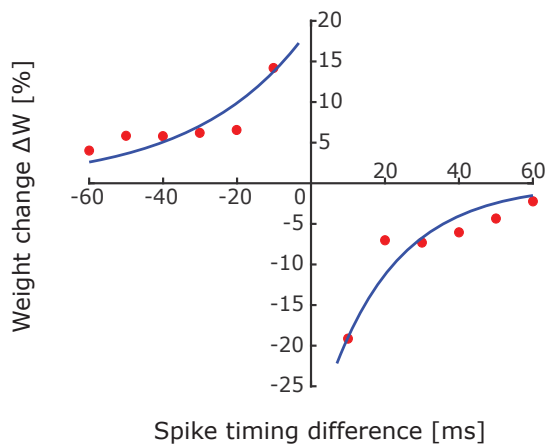


Fig. 7: Anti-Hebbian STDP for GNR synapse shape from Figure 6 (b).

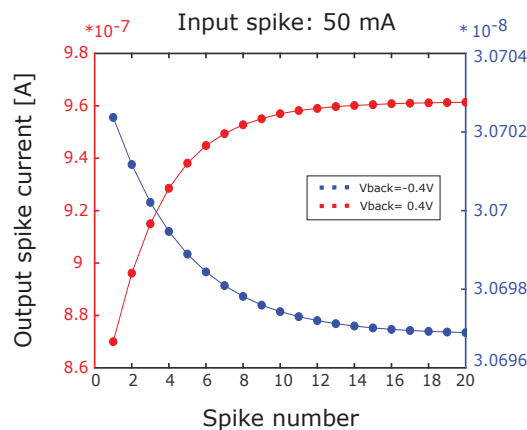


Fig. 8: Output spike current for long-term plasticity.

by the graphene synapse (e.g., S_j^{out} in Figure 1). The long lasting potentiation and depression are successfully emulated for the considered time range with positive and negative back-gate voltage, respectively, as illustrated in Figure 8.

Note that the proposed GNR synapses exhibit a small footprint (e.g., 38 nm^2), and can operate with low voltages, resulting in low energy consumption, which is one of the desired characteristics for large-scale artificial neural network implementations.

V. CONCLUSIONS

In this paper, we proposed and evaluated non-rectangular Graphene Nanoribbon (GNR) based artificial synapses. We demonstrated that by changing the GNR shape and tuning the back-gate voltage, various synaptic plasticity types can be achieved and that the same GNR shape can provide both excitatory and inhibitory synaptic behaviours. We successfully emulated two fundamental synapse functionalities: Spike Timing Dependent Plasticity and Long-Term Plasticity, which underlie learning and memory in brain. We demonstrated that the plasticity can be tuned by changing the GNR synapse shape and topology, thus even though only three STDP types

have been considered the presented GNR synapse design methodology is generic and can be utilized for the design of synapses able to provide other plasticity types. All the simulations have been performed with biologically plausible settings, which indicates that GNR based biologically compatible synapses can be designed, fabricated, and eventually interfaced with biological neurons. The proposed synapses have a small area footprint (order of 10 nm^2) and operate at low operating voltages (order of 100 mV), which makes them strong candidates for the potential implementation of large-scale energy effective artificial neural networks.

REFERENCES

- [1] C. Mead, "Neuromorphic electronic systems," *Proceedings of the IEEE*, vol. 78, no. 10, pp. 1629–1636, 1990.
- [2] P. U. Diehl and M. Cook, "Unsupervised learning of digit recognition using spike-timing-dependent plasticity," *Frontiers in Computational Neuroscience*, vol. 9, p. 99, 2015.
- [3] K. Boahen, "Neuromorphic microchips," *Scientific American*, vol. 292, no. 5, pp. 56–63, 2005.
- [4] W. Gerstner and W. M. Kistler, *Spiking neuron models: Single neurons, populations, plasticity*. Cambridge University Press, 2002.
- [5] S. B. Furber, D. R. Lester, L. A. Plana, J. D. Garside, E. Painkras, S. Temple, and A. D. Brown, "Overview of the spinnaker system architecture," *IEEE Transactions on Computers*, vol. 62, no. 12, pp. 2454–2467, 2013.
- [6] P. A. Merolla, J. V. Arthur, R. Alvarez-Icaza, A. S. Cassidy, J. Sawada, F. Akopyan, B. L. Jackson, N. Imam, C. Guo, Y. Nakamura *et al.*, "A million spiking-neuron integrated circuit with a scalable communication network and interface," *Science*, vol. 345, no. 6197, pp. 668–673, 2014.
- [7] D. B. Strukov, G. S. Snider, D. R. Stewart, and R. S. Williams, "The missing memristor found," *Nature*, vol. 453, no. 7191, p. 80, 2008.
- [8] B. Linares-Barranco and T. Serrano-Gotarredona, "Memristance can explain spike-time-dependent-plasticity in neural synapses," 2009.
- [9] S. Saighi, C. G. Mayr, T. Serrano-Gotarredona, H. Schmidt, G. Lecerf, J. Tomas, J. Grollier, S. Boyn, A. F. Vincent, D. Querlioz *et al.*, "Plasticity in memristive devices for spiking neural networks," *Frontiers in Neuroscience*, vol. 9, p. 51, 2015.
- [10] P. Avouris and C. Dimitrakopoulos, "Graphene: synthesis and applications," *Materials Today*, vol. 15, no. 3, pp. 86–97, 2012.
- [11] M. J. Allen, V. C. Tung, and R. B. Kaner, "Honeycomb carbon: a review of graphene," *Chemical Reviews*, vol. 110, no. 1, pp. 132–145, 2009.
- [12] S. Garaj, W. Hubbard, A. Reina, J. Kong, D. Branton, and J. Golovchenko, "Graphene as a subnanometre trans-electrode membrane," *Nature*, vol. 467, no. 7312, p. 190, 2010.
- [13] H. Tian, W. Mi, X.-F. Wang, H. Zhao, Q.-Y. Xie, C. Li, Y.-X. Li, Y. Yang, and T.-L. Ren, "Graphene dynamic synapse with modulatable plasticity," *Nano Letters*, vol. 15, no. 12, pp. 8013–8019, 2015.
- [14] M. T. Sharbati, Y. Du, J. Torres, N. D. Ardolino, M. Yun, and F. Xiong, "Low-power, electrochemically tunable graphene synapses for neuromorphic computing," *Advanced Materials*, vol. 30, no. 36, p. 1802353, 2018.
- [15] D. E. Feldman, "The spike-timing dependence of plasticity," *Neuron*, vol. 75, no. 4, pp. 556–571, 2012.
- [16] G.-q. Bi and M.-m. Poo, "Synaptic modifications in cultured hippocampal neurons: dependence on spike timing, synaptic strength, and postsynaptic cell type," *Journal of Neuroscience*, vol. 18, no. 24, pp. 10464–10472, 1998.
- [17] H. Wang, N. Cucu Laurenciu, and S. Cotozana, "Atomistic-level hysteresis-aware graphene structures electron transport model," *International Symposium on Circuits and Systems (ISCAS)*, 2019.
- [18] M. G. Reuter and J. C. Hill, "An efficient, block-by-block algorithm for inverting a block tridiagonal, nearly block toeplitz matrix," *Computational Science & Discovery*, vol. 5, no. 1, p. 014009, 2012.
- [19] R. C. Froemke, M.-m. Poo, and Y. Dan, "Spike-timing-dependent synaptic plasticity depends on dendritic location," *Nature*, vol. 434, no. 7030, p. 221, 2005.
- [20] C. Hartmann, D. C. Miner, and J. Triesch, "Precise synaptic efficacy alignment suggests potentiation dominated learning," *Frontiers in Neural Circuits*, vol. 9, p. 90, 2016.